

Global universe anisotropy probed by the alignment of structures in the cosmic microwave background

Y. Wiaux,^{1,*} P. Vielva,^{2,†} E. Martínez-González,² and P. Vandergheynst¹

¹*Signal Processing Institute, Ecole Polytechnique Fédérale de Lausanne (EPFL), CH-1015 Lausanne, Switzerland*

²*Instituto de Física de Cantabria (CSIC-UC), E-39005 Santander, Spain*

We question the global universe isotropy by probing the alignment of local structures in the cosmic microwave background (CMB) radiation. The original method proposed relies on a steerable wavelet decomposition of the CMB signal on the sphere. The analysis of the first-year WMAP data identifies a mean preferred plane with a normal direction close to the CMB dipole axis, and a mean preferred direction in this plane, very close to the ecliptic poles axis. Previous statistical anisotropy results are thereby synthesized, but further analyses are still required to establish their origin.

PACS numbers: 98.70.Vc, 98.80.Es

INTRODUCTION

Last years' experiments in cosmology have resulted in the definition of a consistent picture of the structure and evolution of the universe. The recent data of the cosmic microwave background (CMB) radiation, together with other cosmological observations, have allowed us to determine precise values for the main cosmological parameters [1]. However, the corresponding concordance cosmological model is based on strong hypotheses which need to be questioned. They extend from the nature of the gravitational interaction underpinning the cosmological evolution of the universe, to the physics governing the early inflationary era, or also to the cosmological principle for the global homogeneity and isotropy of the universe.

This letter defines an original method to test the global universe isotropy through the analysis of the CMB data. The observed CMB anisotropies on the celestial sphere can be interpreted as a realization of a statistical process originating in the inflationary era. The cosmological principle implies the isotropy of the corresponding statistical properties. This statistical isotropy has been challenged through multiple methods applied to the first year full-sky CMB data of the Wilkinson Microwave Anisotropy Probe (WMAP) experiment. The detections quoted in the following suggest statistical anisotropy with confidence levels higher than 99 percent. Analyses based on N-point correlation functions [2, 3], local curvature [4], local power spectra [5, 6, 7, 8], and bispectra [9], suggest a north-south asymmetry maximized in a coordinate system with the north pole at $(\theta, \varphi) = (80^\circ, 57^\circ)$ in Galactic co-latitude θ and longitude φ , close to the north ecliptic pole lying at $(\theta, \varphi) = (60^\circ, 96^\circ)$. Analyses of multipole vectors, angular momentum dispersion, as well as azimuthal phases correlations find an anomalous alignment between the low l multipoles of the CMB, suggesting a preferred direction around $(\theta, \varphi) = (30^\circ, 260^\circ)$, near the ecliptic plane and close to the axis of the dipole lying at $(\theta, \varphi) = (42^\circ, 264^\circ)$ [10, 11, 12, 13, 14, 15, 16, 17]. Galactic north-south asymmetries are also found in the

analysis of the kurtosis and the area of the wavelet coefficients of the CMB data. These are mainly due to a very cold spot in the southern hemisphere [18, 19]. First results with the angular pair separation method, which probes the statistical isotropy both in real and multipole space, also seem to support those results [20]. On the contrary, bipolar power spectra analyses are consistent with no violation of the statistical isotropy of the universe [21, 22, 23]. Finally, theoretical models for an anisotropic universe are being studied to account for the observed effects [24].

Our alternative method probes the statistical isotropy of the CMB by the analysis of the alignment of structures in the signal. Preferred directions in the universe are defined as the directions towards which local features of the CMB are mostly oriented. The level of preference of each direction may be established from simulations, and is represented as a signal on the sphere. The approach is therefore powerful as it also *a priori* allows the study of the corresponding angular power spectrum in order to probe the multipole distribution of the anisotropy. The analysis defined relies on a steerable wavelet decomposition of the first year full-sky WMAP data.

DATA AND SIMULATIONS

The experimental temperature map used for the analysis is obtained from the first year WMAP data following the procedure originally proposed in [25] for gaussianity tests. First, a best estimation of diffuse galactic foregrounds is removed from each of the eight frequency maps of the WMAP receivers at the Q , V , and W bands, as prescribed by the specific template fits method in [26]. The eight foreground cleaned maps are then combined through a noise-weighted linear combination in order to enhance the CMB signal-to-noise ratio. The so-called Kp0 mask of [26] is applied to account for the remaining strong foreground contamination by diffuse galactic emissions around the galactic plane and by bright point sources. Finally, the residual monopole and dipole are

subtracted outside the mask. All the WMAP data are released in the HEALPix pixelization on the sphere [27], at a resolution identified by the parameter $N_{side} = 512$, corresponding to maps with several million pixels with a spatial resolution of 6.9 arcminutes. The temperature map obtained from the above pre-processing is downgraded to a lower resolution with $N_{side} = 32$ for the specific purpose of our analysis. This provides a map with $N_{pix} = 12288$ pixels with a spatial resolution of 1.8 degrees.

Ten thousand temperature map simulations at the resolution $N_{side} = 32$ are used in order to define confidence levels for the analysis results. These simulations specifically assume the gaussianity and statistical isotropy of the CMB. They are generated following the scheme also proposed in [25]. A gaussian CMB simulation is obtained in spherical harmonics space from the angular power spectrum determined by the cosmological parameters of the WMAP best-fit cosmological model. The observation at each receiver is simulated by convolving that map with the corresponding WMAP beam window function. After transforming each map to pixel space, a gaussian noise realization is also added with the proper dispersion per pixel. Following the same procedure as for the data, each one of the simulated frequency maps of the eight receivers at the Q , V , and W bands are finally combined through the noise-weighted linear combination which enhances the CMB signal-to-noise ratio, the Kp0 mask is applied, and the monopole and dipole are subtracted.

WAVELET FILTERING

We recall the recently introduced steerable wavelet decomposition of a signal on the sphere upon which we base our analysis.

Let the function $F(\omega)$ describe a signal on the sphere, with the point $\omega = (\theta, \varphi)$ identified by its co-latitude $\theta \in [0, \pi]$ and longitude $\varphi \in [0, 2\pi)$. A wavelet on the sphere is a localized function Ψ that can be dilated at any scale $a \in \mathbb{R}_+^*$ associated with a given angular opening on the sphere, rotated on itself by any angle $\chi \in [0, 2\pi)$, and finally translated at any position $\omega_0 = (\theta_0, \varphi_0)$. The wavelet filtering of F by Ψ results from the scalar product (correlation) of the signal with all the dilated, rotated, and translated versions of the wavelet: $\Psi_{\omega_0, \chi, a}$. Hence, the wavelet coefficients $W_{\Psi}^F(\omega_0, \chi, a) = \langle \Psi_{\omega_0, \chi, a} | F \rangle$ characterize the signal locally at each scale a , in each orientation χ , and at each point ω_0 [28, 29]. Individualizing the properties of the signal independently at each scale is a major advantage of the wavelet scale-space filtering as physical phenomena may generally be scale dependent. Determining the local orientations of the signal structure at each scale also provides essential information for our particular analysis.

Notice that the computation of all wavelet coefficients

for a large number of scales, and with the same high resolution in local orientation and position is a numerically complex calculation. A corresponding fast directional correlation algorithm on the sphere was recently defined which strongly relies on the use of so-called steerable wavelet filters [30]. Our analysis of the WMAP data is performed independently with the first and second gaussian derivatives. These steerable filters, represented in Mollweide projection in figure 1, are analytically defined in [29, 30].



Figure 1: Mollweide projections of the first (left) and second (right) gaussian derivative wavelets at position $\omega_0 = (\pi/2, 0)$, orientation $\chi = 0$, and scale $a = 0.19$. Red and blue regions respectively correspond to positive and negative values.

ANALYSIS METHOD

Here, we consider the analysis leading to the identification of preferred directions from the first year full-sky WMAP data at the HEALPix resolution $N_{side} = 32$. The complementary study of the corresponding angular power spectrum is postponed to a future work.

For a given scale a , the angular size of our wavelets on the sphere is defined as twice the dispersion of the corresponding gaussian. Twelve scales are selected corresponding to angular sizes of the first and second gaussian derivatives lying between 5 and 30 degrees. At each scale, an extended exclusion mask M_a is defined in order to avoid considering pixels for which the correlation between the WMAP signal and the wavelet is contaminated by the Kp0 mask. The pixels added to the initial mask are those for which the wavelet coefficients of a constant signal in the region of the mask are non-zero, up to a given threshold.

For each pixel ω_0 of the signal outside the extended exclusion mask, the direction $\chi_0(\omega_0)$ for which the wavelet coefficient is maximum in absolute value is selected, and the corresponding absolute value is retained. This selects the local wavelet orientation which best matches the orientation of the local structure of the signal at each point. The great circle is defined which passes through that point and admits the corresponding local orientation as a tangent. The directions in the sky lying on that great circle are considered to be highlighted by the local structure identified, and are weighted by the absolute value of the wavelet coefficient $|W_{\Psi}^F(\omega_0, \chi_0(\omega_0), a)|$.

Consider each direction ω on the celestial sphere in the set S of the $N_{pix} = 12288$ pixels at $N_{side} = 32$. The

total weight $D_a(\omega)$ at scale a is the sum of the $N_{cross}(\omega)$ weights originating from all pixels $\omega_0^{(c)}$ in the original signal, with $1 \leq c \leq N_{cross}(\omega)$, for which the great circle defined crosses the direction considered:

$$D_a(\omega) = \frac{1}{A} \sum_{c=1}^{N_{cross}(\omega)} |W_{\Psi}^F(\omega_0^{(c)}, \chi_0(\omega_0^{(c)}), a)|. \quad (1)$$

The factor $A = LN_{pix}^{-1} \sum_{\omega_0 \notin M_a} |W_{\Psi}^F(\omega_0, \chi_0(\omega_0), a)|$ of normalization defines a mean total weight in each direction equal to unity for isotropic CMB simulations without mask: $N_{pix}^{-1} \sum_{\omega \in S} D_a(\omega) = 1$. The quantity $L = 4N_{side}$ stands for the number of points on a great circle on a HEALPix grid. Preferred directions in the universe are therefore identified as the most weighted ones. Notice that the procedure obviously assigns identical total weights to opposite directions. In other words, our directions are headless vectors.

RESULTS

In this section, the results of the analysis of the first year WMAP data proposed above are exposed. The filtering of the CMB data by the first gaussian derivative does not lead to any significant detection. This suggests that there is no clear alignment of the local CMB structures with the morphology captured by that specific filter. The corresponding analysis with the second gaussian derivative leads to a strong detection, detailed in the following.

At each scale a and at each pixel ω , the total weight obtained can be quantified by the number of standard deviations $\sigma_a(\omega)$ through which it deviates from the mean $\mu_a(\omega)$, as estimated from the simulations. Preferred directions, or positive total weights, correspond to $D_a(\omega) > \mu_a(\omega)$. Non-preferred directions, or negative total weights, are distinguished as $D_a(\omega) < \mu_a(\omega)$. We consider in particular the scale a_3 associated with an angular size of the filter of 8.3 degrees on the sky. The corresponding map of total weights clearly depicts the distribution of anisotropy resulting from our analysis (figure 2, top panel).

A rare detection is observed at that specific scale. It identifies 20 directions (pairs of opposite points), qualified as anomalous at 99.99 percent, with an associated positive total weight higher than in any of the ten thousand simulations considered. The 20 anomalous directions obtained at scale a_3 , with positive total weights lying in the interval $[4.4, 7.4]$ in $\sigma_{a_3}(\omega)$ units, are mainly concentrated in two clusters around the ecliptic poles (figure 2, bottom panel). The most prominent of these concentrations comprises 16 of the 20 anomalous directions. Its mean position is identified by a northern end at $(\theta, \varphi) = (71^\circ, 91^\circ)$ in galactic co-latitude θ and longitude φ , when each direction is weighted by its corresponding

total weight. This defines a mean preferred direction in the sky with a northern end very close to the north ecliptic pole at $(\theta, \varphi) = (60^\circ, 96^\circ)$. The presence of the two elongated clusters also suggests that the 20 anomalous directions lie on a great circle, defining a preferred plane in the sky. The normal direction to the mean preferred plane, given by the cross-product of the mean directions of each of the two clusters, has a northern end position at $(\theta, \varphi) = (34^\circ, 331^\circ)$. Alternatively, the great circle which best fits the 20 anomalous directions identifies exactly the same plane. This normal direction lies close to the northern end of the CMB dipole axis at $(\theta, \varphi) = (42^\circ, 264^\circ)$.

Let us emphasize that 11 directions anomalous at 99.99 percent are also detected at the neighbour scale a_4 corresponding to an angular size of the filter of 10 degrees. They belong to two clusters with very similar mean positions to those identified at scale a_3 , and therefore single out the same structure of anisotropy.

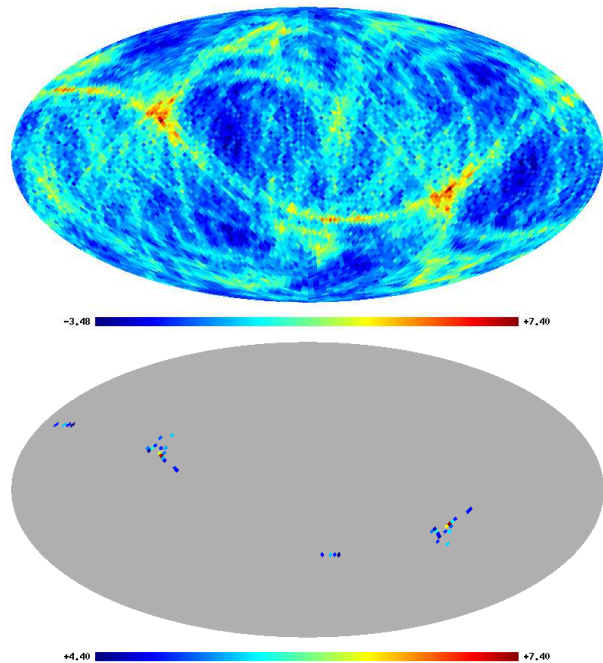


Figure 2: Mollweide projection of the galactic coordinates maps of total weights (top) and directions anomalous at 99.99 percent (bottom) at the scale a_3 of the second gaussian derivative wavelet, and in σ_{a_3} units.

DISCUSSION AND CONCLUSION

The present original analysis of structures alignment in the CMB from the first year WMAP data clearly identifies a mean preferred plane in the universe with a normal direction close to the CMB dipole axis, and a mean preferred direction in this plane, very close to the ecliptic poles axis. This result is based on the observation of 20 directions anomalous at 99.99 percent. Our

original method thus singles out the same directions as those highlighted by previous statistical isotropy studies. The wavelet approach also identifies the angular size of the anomalously aligned structures around 8.3 degrees on the celestial sphere, corresponding to a multipole range roughly between $l = 11$ and $l = 27$.

This new insight into the anisotropy structure might help us to understand its still unclear origin. First, the angular size identified for the aligned structures is compatible with the size of primary CMB anisotropies due to topological defects such as texture fields [31] or secondary anisotropies due to the Rees-Sciama effect [32]. Alignment mechanisms [33, 34] were recently proposed which might be generalized to such structures. Second, the identified angular size is also compatible with the one above which diffuse galactic emissions dominate the CMB emission. Corresponding residual foregrounds can be probed by a direct analysis of the WMAP Q , V , and W bands frequency maps. Finally, the coincidence of the preferred directions detected with the ecliptic poles and dipole axes naturally suggests possible unknown systematic effects [33, 35]. In that respect, notice that the angular size of the mesh of the WMAP scan pattern defined by the combination of the spin and precession of the satellite is, again, of the order of several degrees [36].

In conclusion, our analysis provides a first synthesis of previous statistical anisotropy results. Further analyses of the complete total weights distributions at various wavelet scales and of the corresponding angular power spectra can allow a deeper probe of the anisotropy structure. But the origin of the present detection already needs to be thoroughly investigated. Various hypotheses can be suggested in terms of cosmological or foreground structures, or systematics. But nothing at present allows us to discard the possibility of a global universe anisotropy, simple violation of the cosmological principle hypothesis.

The authors acknowledge the use of the LAMBDA archive, and of the HEALPix and CMBFAST softwares. Y. W. was supported by the Swiss and Belgian National Science Foundations. P. V. and E. M.-G. were supported by the Spanish MEC project ESP2004-07067-C03-01.

* Electronic address: yves.wiaux@epfl.ch

† Electronic address: vielva@ifca.unican.es

- [1] D. N. Spergel *et al.*, *Astrophys. J. Suppl.* **148**, 175 (2003).
- [2] H. K. Eriksen, F. K. Hansen, A. J. Banday, K. M. Górski, and P. B. Lilje, *Astrophys. J.* **605**, 14 (2004).
- [3] H. K. Eriksen, A. J. Banday, K. M. Górski, and P. B. Lilje, *Astrophys. J.* **622**, 58 (2005).
- [4] F. K. Hansen, P. Cabella, D. Marinucci, and N. Vittorio, *Astrophys. J. Lett.* **607**, L67 (2004).
- [5] F. K. Hansen, K. M. Górski, and E. Hivon, *Mon. Not. R. Astron. Soc.* **336**, 1304 (2002).
- [6] F. K. Hansen, A. J. Banday, and K. M. Górski, preprint astro-ph/0404206 (2004).
- [7] F. K. Hansen, A. Balbi, A. J. Banday, and K. M. Górski, preprint astro-ph/0406232 (2004).
- [8] E. P. Donoghue and J. F. Donoghue, *Phys. Rev. D* **71**, 043002 (2005).
- [9] K. Land and J. Magueijo, *Mon. Not. R. Astron. Soc.* **357**, 994 (2005).
- [10] C. J. Copi, D. Huterer, and G. D. Starkman, *Phys. Rev. D* **70**, 043515 (2004).
- [11] G. Katz and J. Weeks, *Phys. Rev. D* **70**, 063527 (2004).
- [12] D. J. Schwarz, G. D. Starkman, D. Huterer, and C. J. Copi, *Phys. Rev. Lett.* **93**, 221301 (2004).
- [13] K. Land and J. Magueijo, *Mon. Not. R. Astron. Soc.* **362**, L16 (2005).
- [14] K. Land and J. Magueijo, *Mon. Not. R. Astron. Soc.* **362**, 838 (2005).
- [15] A. de Oliveira-Costa, M. Tegmark, M. Zaldarriaga, and A. Hamilton, *Phys. Rev. D* **69**, 063516 (2004).
- [16] K. Land and J. Magueijo, *Phys. Rev. Lett.* **95**, 071301 (2005).
- [17] P. Bielewicz, H. K. Eriksen, A. J. Banday, K. M. Górski, and P. B. Lilje, preprint astro-ph/0507186 (2005).
- [18] P. Vielva, E. Martínez-González, R. B. Barreiro, J. L. Sanz, and L. Cayón, *Astrophys. J.* **609**, 22 (2004).
- [19] M. Cruz, E. Martínez-González, P. Vielva, and L. Cayón, *Mon. Not. R. Astron. Soc.* **356**, 29 (2005).
- [20] A. Bernui, B. Mota, M. J. Rebouças, and R. Tavakol, preprint astro-ph/0511666 (2005).
- [21] A. Hajian and T. Souradeep, preprint astro-ph/0501001 (2005).
- [22] A. Hajian and T. Souradeep, *Astrophys. J. Lett.* **597**, L5 (2003).
- [23] A. Hajian, T. Souradeep, and N. Cornish, *Astrophys. J. Lett.* **618**, L63 (2005).
- [24] T. R. Jaffe, A. J. Banday, H. K. Eriksen, K. M. Górski, and F. K. Hansen, *Astrophys. J. Lett.* **629**, L1 (2005).
- [25] E. Komatsu *et al.*, *Astrophys. J. Suppl.* **148**, 119 (2003).
- [26] C. L. Bennet *et al.*, *Astrophys. J. Suppl.* **148**, 97 (2003).
- [27] K. M. Górski, E. Hivon, A. J. Banday, B. D. Wandelt, F. K. Hansen, M. Reinecke, and M. Bartelman, *Astrophys. J.* **622**, 759 (2005).
- [28] J.-P. Antoine and P. Vanderghenst, *J. Math. Phys.* **39**, 3987 (1998).
- [29] Y. Wiaux, L. Jacques, and P. Vanderghenst, *Astrophys. J.* **632**, 15 (2005).
- [30] Y. Wiaux, L. Jacques, and P. Vanderghenst, preprint astro-ph/0508516 (2005).
- [31] N. Turok and D. N. Spergel, *Phys. Rev. Lett.* **64**, 2736 (1990).
- [32] E. Martínez-González and J. L. Sanz, *Mon. Not. R. Astron. Soc.* **247**, 473 (1990).
- [33] C. Gordon, W. Hu, D. Huterer, and T. Crawford, *Phys. Rev. D* **72**, 103002 (2005).
- [34] A. Rakić, S. Räsänen, and D. J. Schwarz, preprint astro-ph/0601445 (2006).
- [35] P. E. Freeman, C. R. Genovese, C. J. Miller, R. C. Nichol, and L. Wasserman, *Astrophys. J.* **638**, 1 (2006).
- [36] C. L. Bennet *et al.*, *Astrophys. J.* **583**, 1 (2003).